

Aggregation in Dilute Aqueous Solutions of Hydroxypropyl Cellulose with Salt Ions

Valery I. Kovalchuk

*Taras Shevchenko National University of Kyiv, Faculty of Physics
(64/13, Volodymyrska Str., Kyiv 01601, Ukraine)*

Thermal behaviors of hydroxypropyl cellulose dilute aqueous solutions with impurities of Group I alkali metal ions (Li, Na, K, Rb and Cs chlorides) has been studied by means of static and dynamic light scattering measurements. From the experimental data, it follows that at temperatures above the LCST and in the presence of salts, there arise supramolecular associates (clusters) that are several times larger than the wavelength of visible light. It is shown that the observed intensity of backscattered light is described by the tangent plane approximation and the Mie scattering theory.

Keywords: static and dynamic light scattering, hydroxypropyl cellulose, salt ions.

1. Introduction

The study of the solutions of cellulose derivatives is based on promising technologies in various fields, including the food industry, construction, hydrocarbon production, aerospace materials, medicine and pharmaceuticals [1–3]. A characteristic feature of many water-soluble cellulose ethers is the thermoreversible volume transition [4]. Its essence consists in the formation of a polymer gel network when the temperature increases, but the system returns to the state of isotropic solution when cooled down. The threshold temperature of this transition is called the lower critical solution temperature (LCST) which depends on a number of factors such as polymer concentration, type and degree of substitution [5–7], pH value [8–11], and the presence of electrolytes in solution [12–16].

A number of works are devoted to the study of the thermosensitive behavior of cellulose derivatives aqueous solutions with salt ions [12–14, 17–22]. The main

methods that were used: turbidimetry [14, 18, 19, 22], dynamic light scattering (DLS) [17, 19, 21, 22], microcalorimetry [12–14, 18], and viscometry [13, 14, 18, 20–22]. In the articles listed above the volume phase transition mechanisms were mainly studied depending on the type of salt additives and their concentration. In particular, it was shown that the thermosensitive behavior of polymer solution is based on competition for water molecules between polymer chains and salt ions, which leads to the hydrophobic aggregates formation [12–15].

It should be noted that ions can act as aggregation initiators not only in solutions of cellulose derivatives, but also in other systems containing, for example, peptides [23], pseudo-polypeptoids [24], lignin [25], lipid nanoparticles [26], latex particles [27, 28], and silica particles [29]. In general, the study of aggregation in polymer solutions is of great practical importance for modern technologies, such as catalysts with controlled activity and film nanocomposite materials [30–32], color-based sensors that respond to pH and heavy metal ions [33], energy-saving smart windows [34, 35], and drug delivery systems [8, 9].

Hydroxypropyl cellulose (HPC) as an object of research was chosen due to the attractiveness of its physical and chemical properties. In addition to the well-known unique properties of a green polymer, such as availability, cheapness, and biocompatibility, HPC has a low LCST value of $(40 \div 45)^\circ\text{C}$ [7–9, 34–37]. Such a temperature makes HPC a good choice for both biomedical applications and promising smart technologies [10]. In our recent work [22], it was found that the addition of salts (chlorides of Group I alkali metal ions) to dilute aqueous solutions of HPC leads to polymer aggregation at temperatures above LCST. As a continuation of [22], in this work these same systems are studied using static light scattering. The obtained light backscattering data were analyzed within the framework of the tangent plane approximation and Mie scattering theory.

2. Materials and Methods

2.1. Materials

The cellulose derivative, hydroxypropyl cellulose (HPC), was purchased from Alfa Aesar company. The manufacturer’s specification indicates that HPC has an average degree of substitution of 75.7% and a molecular weight of 100,000. The

viscosity range was reported by the manufacturer to be 112 cPs at 25° C for a 5 wt% aqueous solution.

Analytical grade salts (Li, Na, K, Rb, Cs chlorides) were purchased from Sigma-Aldrich company.

2.2. Specimen Preparation

The initial aqueous HPC solution with a concentration of 2 wt% was prepared by dissolving the necessary amount of polymer in deionized water under continuous stirring for 4 hours at a temperature of 60° C to ensure the complete dissolution of the polymer. As a result, a homogeneous and transparent solution was obtained.

This initial solution was divided to prepare six specimens. The salts were introduced into five of them, and the specimens were mixed until the complete salt dissolution. The molar concentrations of the salt in the specimens were identical and equal to that of the physiological solution (154 mmol/l). By diluting 2% solutions with water to a ratio of 1:10, specimens with a polymer concentration of 0.2 wt% and a salt concentration of 15.4 mmol/l were fabricated.

2.3. Static Light Scattering

The temperature dependences of the intensities of backscattered light were measured on the installation described in works [38,39].

2.4. Dynamic Light Scattering

Particle sizes (hydrodynamic diameters) were determined [22,40] using a Zeta-sizer Nano ZS (Malvern, UK) instrument at 173 deg backscatter geometry. Before measurement, all specimens were dust-removed through a 0.2 um filter (Minisart NML). For each temperature point, the particle size distributions in a given specimen were measured three times.

3. Results and Their Discussion

3.1. Static and Dynamic Light Scattering

The studies were performed using the device described in detail in works [38,39]. When falling on the surface of the examined solution, the primary beam of light with a wavelength of 525 nm formed two beams, transmitted and reflected. The

corresponding intensities J_T and J_R of these beams were measured at a set of temperatures within an interval from 30 to 65° C. The specimen heating rate was 1.1° C/min. The obtained experimental data were calibrated in each specimen to a transparency level of 100%. As such the corresponding value of J_T at a temperature of 30° C was selected.

Figure 1 exhibits the measurement results obtained for the temperature dependences of the relative intensities of the backscattered light beam for all six specimens. The same figure also shows the average size of particles (hydrodynamic diameter, D) determined by the dynamic light scattering method (points) [22, 40].

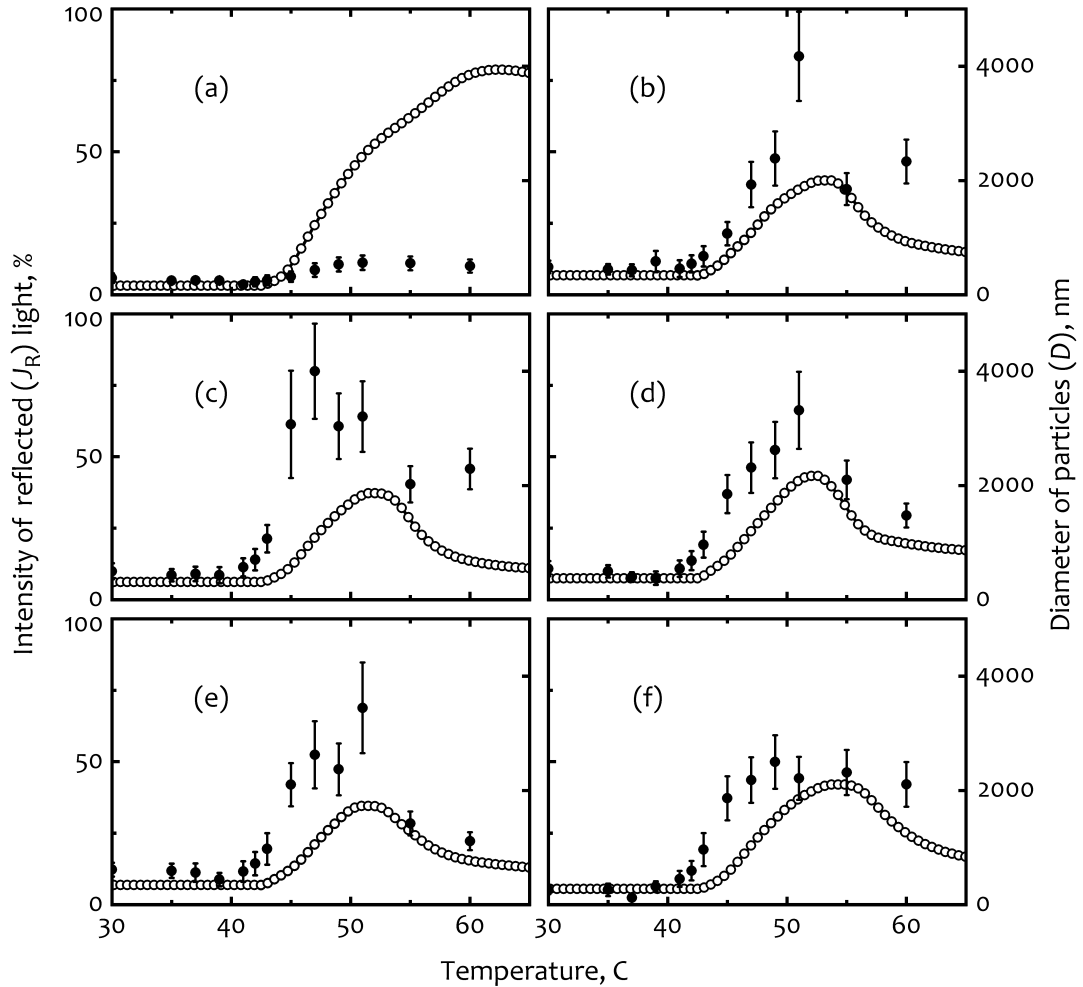


Figure 1: Temperature dependences of the reflected light intensity J_R (left vertical scale, \circ) for specimens: (a) – ion-free, (b) – Li, (c) – Na, (d) – K, (e) – Rb, (f) – Cs. The values of hydrodynamic diameter D are also shown here (right vertical scale, \bullet).

3.2. Light Backscatter Analysis

From Fig. 1, one can see that the experimental dependences $J_R(T)$ for the solution with salt ions has a non-monotonic character: as the temperature increases, the J_R -values first grow, then reach a maximum, and afterward decrease. This behavior can be explained as follows.

The solution surface on which the light falls is not perfectly smooth – it contains polymer inclusions of various sizes, therefore it can be considered as a statistically rough surface. The studies of light scattering by such surfaces have a long (for more than a hundred years) story [41]. It is known that the solution of this problem is reduced to the analysis of a wave equation of a certain type. Instead, in this paper, we will confine ourselves to a qualitative consideration proceeding from assumptions concerning the type of backward scattering, which forms the output beam with the intensity J_R .

Let the solution surface look like a plane on average. Let's draw the z -axis perpendicular to this plane. Surface roughness $z = \xi(r)$ is described by two statistical parameters [42]: parameter δ (root-mean-square height of surface deviation from the plane $z = 0$) and parameter α (lateral correlation length of roughness, describing the average lateral distance between the peak and valley of the surface profile).

We assume that the incident light propagates along the z -axis and that the condition

$$(kR_c)^{1/3} \gg 1 \tag{1}$$

is satisfied. Here k is the modulus of the wave vector of the scattered photon, R_c is the radius of surface curvature, which can be estimated as $R_c = 2\sqrt{3}\alpha^2/\delta$ [43].

Inequality (1) is a condition for the applicability of the tangent plane method, developed in [44] based on the theory of wave scattering by a statistically rough surface [41]. The main conclusions of this method as applied to light backscattering are as follows.

When considering methods for assessing the reflective properties of light by a rough surface, the entire reflected signal is divided into a coherent component and an incoherent one. The coherent component is associated with specular reflection from surface areas and is determined by the average value of the field strength in

the scattered wave. According to [41], the back reflection coefficient of the coherent component for a surface with a normal distribution of heights is equal to

$$\rho = J_{\text{R}}/J_0 = \exp(-2k^2\delta^2), \quad (2)$$

where J_0 is the intensity of incident light beam. From (2) it follows that the value of J_{R} decrease exponentially as the characteristic height of irregularities increases.

It was shown in [41,45] that the cross section for light backscattering by a three-dimensional statistically rough surface is

$$\Sigma \sim Na^2, \quad (3)$$

where N is the number of scattering centers (points of specular reflection, which correspond to the peaks and valleys of the surface $z = \xi(r)$), and the value a is the geometric mean of the main radii of curvature a_1 and a_2 at the points of specular reflection

$$a^2 = \langle a_1 a_2 \rangle. \quad (4)$$

Formula (3) has a simple geometric meaning: the scattering cross section by a rough surface in the tangent plane approximation (1) coincides with the scattering cross section by N identical balls with radius a . Consequently, the problem of light scattering by a statistically rough surface can be reduced to the equivalent problem of scattering by a system of spherical particles. Since the amount of polymer in the solution is a constant parameter, the number of such particles equals

$$N \sim 1/a^3, \quad (5)$$

and, therefore,

$$\Sigma \sim 1/a. \quad (6)$$

Note that the result (6) can also be obtained within the framework of the Mie scattering theory [46]. The Mie backscattering cross section for a single particle has the form [47]

$$\sigma(a) = \frac{1}{a^2 k^2} \left| \sum_{n=1}^{\infty} (-1)^n (2n+1) (A_n(a, k) - B_n(a, k)) \right|^2, \quad (7)$$

where A_n , B_n are the Mie coefficients [48].

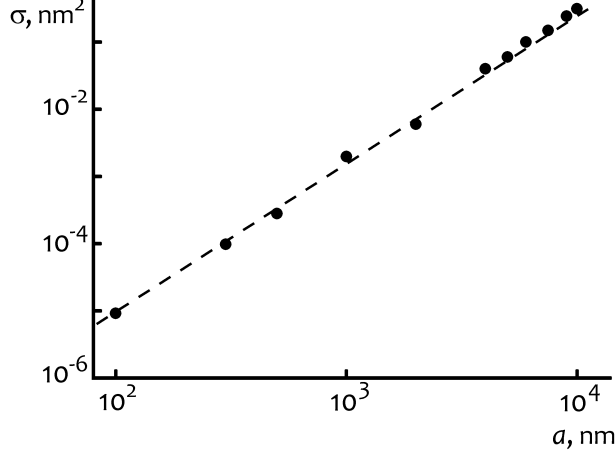


Figure 2: Mie backscattering cross section for a single spherical aggregate of hydroxypropyl cellulose with radius a (set of black dots).

Figure 2 shows the results of calculating the cross section (7). Calculations were performed according to the method of [49, 50] for light with a wavelength of 525 nm and the refractive index value taken from [51] for the aqueous HPC solution.

This figure shows that the $\sigma(a)$ dependence has the scaling behavior (dashed line)

$$\sigma(a) \sim a^s \quad (8)$$

with the power exponent $s = 2$. Hence, the total cross section of Mie backscattering for N identical spherical particles, taking into account (5), is

$$\Sigma_{\text{Mie}} \sim Na^2 = 1/a, \quad (9)$$

which coincides with the formula (6). It follows from formula (9) that

$$J_{\text{R}} \sim 1/a, \quad (10)$$

that is, the intensity of backscattered light increases as the particle size decreases. The same conclusion can be drawn, if we compare the experimental values of J_{R} and D (see Fig. 1b-f).

As mentioned above, the behavior of $J_{\text{R}}(T)$ in Fig. 1b-f has a non-monotonic character: as the temperature increases, the J_{R} -values first grow, then reach a maximum at $T' \simeq (50 \div 55)^\circ \text{C}$, and afterward decrease. The sizes of the polymer clusters (see the same figures) have a similar temperature behavior. There are two explanations for the decrease of cluster sizes at $T > T'$. The first of them consists in

that the clusters collapse at $T > T'$ and form numerous small fragments. But in this case, as follows from Eq.(10), instead of the reduction of the intensity J_R , we would observe its growth, which contradicts the experiment. The second explanation is that large polymer aggregates disappear from the solution at $T > T'$ owing to their sedimentation, which is confirmed by the experiment: whenever the measurements were concluded, some polymer sediment was found at the bottom of the cell with the solution. This sediment did not dissolve well in a hot solution, but it dissolved easily in cold water.

Note that the viscosity of the 0.2-wt% aqueous solutions of HPC at $(50 \div 60)^\circ\text{C}$ exceeds the viscosity of water by only 5–7% [21]. Therefore, the sedimentation of polymer clusters occurred quite quickly: from Fig. 1b-f, it follows that J_R decreased by a factor of two during about 10 min.

Figure 1 also demonstrates that the sizes D of clusters in the ion-free specimen are several times smaller than in the specimen with ions. By order of magnitude, they are equal to the wavelength of visible light. In Fig.1a, the intensity of reflected light is larger than that in Fig. 1b-f, as it should be according to formula (10). The polymer clusters in the ion-free solution were in a suspended state, and practically no sediment was observed in the cell after the measurements.

4. Conclusions

Using the methods of static and dynamic light scattering, dilute aqueous solutions of HPC (0.2 wt%) with the admixtures of Group I alkali metal chlorides (15.4 mmol/l) are studied. It is found that, at temperatures higher than the LCST, there arises inverse scattering of light via the light reflection from the supramolecular structure of the researched solutions. In the solutions with ions, there emerge large macromolecular associations (clusters) whose size is several times larger than the wavelength of visible light. The temperature dependence of the intensity J_R of backward scattering is non-monotonic for specimens with salts; namely, as the temperature grows, the values of J_R increase, reach a maximum, and finally decrease. The hydrodynamic diameter of clusters is demonstrated the same behavior in corresponding solutions with ions, correlating with the J_R -values. There is a relation between the values of J_R and the sizes of polymer clusters, which was found in the

framework of the tangent plane approximation and Mie scattering theory. In particular, it is shown that the reduction of $J_R(T)$ in an interval of $(55 \div 65)^\circ \text{C}$ occurs due to the sedimentation of clusters rather than their decay, which was confirmed experimentally. This study may provide useful information for the development of polymer films with a given structure and characteristics, as well as new drug delivery systems.

REFERENCES

1. Okano, T. *Biorelated Polymers and Gels: Controlled Release and Applications in Biomedical Engineering (Polymers, Interfaces and Biomaterials)*, 1st ed.; Academic Press: Cambridge, Massachusetts, USA, 1998; ISBN 978-0125250900.
2. Kamide, K. *Cellulose and Cellulose Derivatives: Molecular Characterization and its Applications*, 1st ed.; Elsevier Science: Amsterdam, Netherlands, 2005; ISBN 978-0080454443.
3. Kabir, S.M.F.; Sikdar, P.P.; Haque, B.; Bhuiyan, M.A.R.; Ali, A.; Islam, M.N. Cellulose-based hydrogel materials: chemistry, properties and their prospective applications. *Prog. Biomater.* **2018**, *7*, 153–174. [DOI: 10.1007/s40204-018-0095-0].
4. Tanaka, F. *Polymer Physics: Applications to Molecular Association and Thermoreversible Gelation*; Cambridge University Press: Cambridge, UK, 2011. [DOI: 10.1017/CBO9780511975691].
5. Bayer, R.; Knarr, M. Thermal precipitation or gelling behaviour of dissolved methylcellulose (MC) derivatives—Behaviour in water and influence on the extrusion of ceramic pastes. Part 1: Fundamentals of MC-derivatives. *J. Eur. Ceram. Soc.* **2012**, *32*, 1007-1018. [DOI: 10.1016/j.jeurceramsoc.2011.11.025].
6. Tian, Y.; Liu, Y.; Ju, B.; Ren, X., Dai, M. Thermoresponsive 2-hydroxy-3-isopropoxypropyl hydroxyethyl cellulose with tunable LCST for drug delivery. *RSC Adv.* **2019**, *9*, 2268–2276. [DOI: 10.1039/c8ra09075k].
7. Gosecki, M; Setälä, H.; Virtanen, T.; Ryan, A.J. A facile method to control the phase behavior of hydroxypropyl cellulose. *Carbohydr. Polym.* **2021**, *251*, 117015(7pp). [DOI: 10.1016/j.carbpol.2020.117015].

8. Zhang, Z.; Chen, L.; Zhao, C.; Bai, Y.; Deng, M.; Shan, H.; Zhuang, X.; Chen, X.; Jing, X. Thermo- and pH-responsive HPC-g-AA/AA hydrogels for controlled drug delivery applications. *Polymer* **2011**, *52*, 676–682. [DOI: 10.1016/j.polymer.2010.12.048].
9. Bai, Y.; Zhang, Z.; Zhang, A.; Chen, L.; He, C.; Zhuang, X.; Chen, X. Novel thermo- and pH-responsive hydroxypropyl cellulose- and poly (l-glutamic acid)-based microgels for oral insulin controlled release. *Carbohydr. Polym.* **2012**, *89*, 1207–1214. [DOI: 10.1016/j.carbpol.2012.03.095].
10. Qiu, X.; Hu, S. “Smart” Materials Based on Cellulose: A Review of the Preparations, Properties, and Applications. *Materials* **2013**, *6*, 738–781. [DOI: 10.3390/ma6030738].
11. Ofriidam, F.; Tarhini, M.; Lebaz, N.; Gagnière, É.; Mangin, D.; Elaissari, A. pH-sensitive polymers: Classification and some fine potential applications. *Polym. Adv. Technol.* **2021**, *32*, 1455–1484. [DOI: 10.1002/pat.5230].
12. Xu, Y.; Wang, C.; Tam, K.C.; Li, L. Salt-Assisted and Salt-Suppressed Sol-Gel Transitions of Methylcellulose in Water. *Langmuir* **2004**, *20*, 646–652. [DOI: 10.1021/la0356295].
13. Xu, Y.; Li, L.; Zheng, P.; Lam, Y.C.; Hu, X. Controllable Gelation of Methylcellulose by a Salt Mixture. *Langmuir* **2004**, *20*, 6134–6138. [DOI: 10.1021/la049907r].
14. Zheng, P.; Li, L.; Hu, X.; Zhao, X. Sol–Gel Transition of Methylcellulose in Phosphate Buffer Saline Solutions. *J. Polym. Sci. B Polym. Phys.* **2004**, *42*, 1849–1860. [DOI: 10.1002/polb.20070].
15. Liu, S.Q.; Joshi, S.C.; Lam, Y.C. Effects of salts in the Hofmeister series and solvent isotopes on the gelation mechanisms for hydroxypropylmethylcellulose hydrogels. *J. Appl. Polym. Sci.* **2008**, *109*, 363–372. [DOI: 10.1002/app.28079].
16. Weißenborn, E.; Braunschweig, B. Hydroxypropyl cellulose as a green polymer for thermo-responsive aqueous foams. *Soft Matter* **2019**, *15*, 2876–2883. [DOI: 10.1039/c9sm00093c].
17. Nyström, B.; Roots, J.; Carlsson, A.; Lindman, B. Light scattering studies of the gelation process in an aqueous system of a non-ionic polymer and a cationic surfactant. *Polymer* **1992**, *33*, 2875–2882. [DOI: 10.1016/0032-3861(92)90071-4].

18. Joshi, S.C. Sol-Gel Behavior of Hydroxypropyl Methylcellulose (HPMC) in Ionic Media Including Drug Release. *Materials* **2011**, *4*, 1861-1905. [DOI: 10.3390/ma4101861].
19. Fettaka, M.; Issaadi, R.; Moulai-Mostefa, N.; Dez, I.; Le Cerf, D.; Picton, L. Thermo sensitive behavior of cellulose derivatives in dilute aqueous solutions: From macroscopic to mesoscopic scale. *J. Colloid Interface Sci.* **2011**, *357*, 372-378. [DOI: 10.1016/j.jcis.2011.02.041].
20. Almeida, N.; Rakesh, L.; Zhao, J. Monovalent and divalent salt effects on thermogelation of aqueous hypromellose solutions. *Food Hydrocoll.* **2014**, *36*, 323-331. [DOI: 10.1016/j.foodhyd.2013.10.020].
21. Lazarenko M.; Nedilko S.; Gryn S.; Scherbatskyi V.; Kovalchuk V.; Lazarenko M.; Sobchuk A.; Andrusenko D.; Alekseev O. Influence of Na⁺ and Cl⁻ Ions on the Properties of Hydroxypropyl Cellulose Solutions. In Proceedings of the 2022 IEEE 41st International Conference on Electronics and Nanotechnology (ELNANO), Kyiv, Ukraine, October 10-14, 2022. [DOI: 10.1109/ELNANO54667.2022.9927040].
22. Lazarenko, M.M.; Alekseev, O.M.; Nedilko, S.G.; Sobchuk, A.O.; Kovalchuk, V.I.; Gryn, S.V.; Scherbatskyi, V.P.; Tkachev, S.Yu.; Andrusenko, D.A.; Rudnikov, E.G.; Brytan, A.V.; Yablochkova, K.S.; Lysenkov, E.A.; Dinzhos, R.V.; Sabu, T.; Abraham, T.R. Impact of the Alkali Metals Ions on the Dielectric Relaxation and Phase Transitions in Water Solutions of the Hydroxypropylcellulose. In *NANO 2022: Nanoelectronics, Nanooptics, Nanochemistry and Nanobiotechnology, and Their Applications*; Fesenko, O., Yatsenko, L., Eds.; Springer Proceedings in Physics: Cham, Switzerland, 2023; Volume 297, pp. 37-68. [DOI: 10.1007/978-3-031-42708-4].
23. Klement, K.; Wieligmann, K.; Meinhardt, J.; Hortschansky, P.; Richter, W.; Fändrich, M. Effect of Different Salt Ions on the Propensity of Aggregation and on the Structure of Alzheimer's A β (1-40) Amyloid Fibrils. *J. Mol. Biol.* **2007**, *373*, 1321-1333. [DOI: 10.1016/j.jmb.2007.08.068].
24. Kirila, T.; Smirnova, A.; Razina, A.; Tenkovtsev, A.; Filippov, A. Influence of Salt on the Self-Organization in Solutions of Star-Shaped Poly-2-alkyl-2-oxazoline and Poly-2-alkyl-2-oxazine on Heating. *Polymers* **2021**, *13*, 1152(15pp). [DOI: 10.3390/polym13071152].

25. Fritz, C.; Salas, C.; Jameel, H.; Rojas, O.J. Self-association and aggregation of kraft lignins via electrolyte and nonionic surfactant regulation: stabilization of lignin particles and effects on filtration. *Nord. Pulp Paper Res. J.* **2017**, *32*, 572-585. [DOI: 10.3183/npprj-2017-32-04_p572-585_rojas].
26. Wei, C.-C.; Ge, Z.-Q. Influence of electrolyte and poloxamer 188 on the aggregation kinetics of solid lipid nanoparticles (SLNs). *Drug Dev. Ind. Pharm.* **2011**, *38*, 1084–1089. [DOI: 10.3109/03639045.2011.640331].
27. Pefferkorn, E. Electrolyte and Poly electrolyte Induced Aggregation of Colloids. Mechanism of Colloid Destabilization. *Croat. Chem. Acta* **1992**, *65*, 309-326. [<https://hrcak.srce.hr/file/202172>].
28. Hanus, L.H.; Hartzler, R.U.; Wagner, N.J. Electrolyte-Induced Aggregation of Acrylic Latex. 1. Dilute Particle Concentrations. *Langmuir* **2001**, *17*, 3136–3147. [DOI: 10.1021/la000927c].
29. Tavecchi, J.W.; Dowding, P.J.; Routh, A.F. The polymer and salt induced aggregation of silica particles. *Colloids Surf. A Physicochem. Eng. Asp.* **2007**, *293*, 167–174. [DOI: 10.1016/j.colsurfa.2006.07.025].
30. Khokhlov, A.R.; Dormidontova, E.E. Self-organization in ion-containing polymer systems. *Phys.-Uspekhi* **1997**, *40*, 109–124. [DOI: 10.1070/PU1997v040n02ABEH000191].
31. Bukhari, S.N.A.; Hussain, M.A.; Shah, A.; Jantan, I.; Shah, M.R.; Tahir, M.N.; Ahmad, R. Hydroxypropylcellulose as a novel green reservoir for the synthesis, stabilization, and storage of silver nanoparticles. *Int. J. Nanomedicine* **2015**, *10*, 2079-2088. [DOI: 10.2147/ijn.s75874].
32. Alharbi, N.D. Synthesis of composites from hydroxypropyl cellulose: iron (III) oxide nanoparticles. *Polym. Polym. Compos.* **2023**, *31*, 1012. [DOI: 10.1177/09673911221149548].
33. Lee, S.-J.; Kumar, S.; Choi, J.W.; Lee, J.-S. Coloration of colloidal polymer particles through selective extraction of Mie backscattering for cation-responsive colorimetric sensors. *J. Colloid Interface Sci.* **2020**, *560*, 894-901. [DOI: 10.1016/j.jcis.2019.10.073].

34. Connelly, K.; Wu, Y.; Ma, X.; Lei, Y. Transmittance and Reflectance Studies of Thermotropic Material for a Novel Building Integrated Concentrating Photovoltaic (BICPV) ‘Smart’ Window System. *Energies* **2017**, *10*, 1889(13pp). [DOI: 10.3390/en10111889].
35. Nakamura, A.; Ogai, R.; Murakami, K. Development of smart window using an hydroxypropyl cellulose-acrylamide hydrogel and evaluation of weathering resistance and heat shielding effect. *Sol. Energy Mater Sol. Cells* **2021**, *232*, 111348(8pp). [DOI: 10.1016/j.solmat.2021.111348].
36. Harsh, D.C.; Gehrke, S.H. Controlling the swelling characteristics of temperature-sensitive cellulose ether hydrogels. *J. Control. Release* **1991**, *17*, 175-186. [DOI: 10.1016/0168-3659(91)90057-K].
37. Narang, A.S.; Badawy, S.I.F. *Handbook of Pharmaceutical Wet Granulation: Theory and Practice in a Quality by Design Paradigm*, 1st ed.; Academic Press: Cambridge, Massachusetts, USA, 2019; ISBN 978-0128104606.
38. Kovalchuk, V.I.; Alekseev, O.M.; Lazarenko, M.M. Turbidimetric Monitoring of Phase Separation in Aqueous Solutions of Thermoresponsive Polymers. *J. Nano- Electron. Phys.* **2022**, *14*, 01004(4pp). [DOI: 10.21272/jnep.14(1).01004].
39. Kovalchuk, V.I. Phase separation dynamics in aqueous solutions of thermoresponsive polymers. *Cond. Matt. Phys.* **2021**, *24*, 43601(9pp). [DOI: 10.5488/CMP.24.43601].
40. Lazarenko, M.M. (Faculty of Physics, Taras Shevchenko National University of Kyiv, Ukraine). Personal communication, 2023.
41. Bass, F.G.; Fuks, I.M. *Wave Scattering from Statistically Rough Surfaces*, 1st ed.; Pergamon Press: Oxford, UK, 1979; ISBN 978-1483187754.
42. Lu, J.Q.; Hu, X.-H.; Dong, K. Modeling of the rough-interface effect on a converging light beam propagating in a skin tissue phantom. *Appl. Opt.* **2000**, *39*, 5890-5897. [DOI: 10.1364/ao.39.005890].
43. Lu, J.Q.; Maradudin, A.A.; Michel, T. Enhanced backscattering from a rough dielectric film on a reflecting substrate. *J. Opt. Soc. Am. B* **1991**, *8*, 311-317. [DOI: 10.1364/JOSAB.8.000311].
44. Voronovich, A.G. Tangent Plane Approximation and Some of Its Generalizations. *Acoust. Phys.* **2007**, *53*, 298-304. [DOI: 10.1134/S1063771007030062].

45. Kodis, R. A Note on the Theory of Scattering from an Irregular Surface. *IEEE Trans. Antennas Propag.* **1966**, *14*, 77–82. [DOI: 10.1109/TAP.1966.1138626].
46. Mie, G. Beiträge zur Optik trüber Medien, speziell kolloidaler Metallösungen. *Ann. Phys.* **1908**, *330*, 377–445. [DOI: 10.1002/andp.19083300302].
47. Tzarouchis, D.; Sihvola, A. Light Scattering by a Dielectric Sphere: Perspectives on the Mie Resonances. *Appl. Sci.* **2018**, *8*, 184–205. [DOI: 10.3390/app8020184].
48. Kerker, M.; Wang, D.S.; Giles, C.L. Electromagnetic scattering by magnetic spheres. *J. Opt. Soc. Am.* **1983**, *73*, 765-767. [DOI: 10.1364/JOSA.73.000765].
49. Mätzler, Ch. *MATLAB Functions for Mie Scattering and Absorption*, ver. 2; Institute of Applied Physics: Bern, Switzerland, 2002; Research Report No. 2002-11.
50. Mie Scattering Calculator. Available online: https://omlc.org/calc/mie_calc.html (accessed on April 10, 2024).
51. Maklakova, A.A.; Kulichikhin, V.G.; Malkin, A.Y. The Formation and Elasticity of a Hydroxypropyl Cellulose Film at a Water-Air Interface. *Colloid J.* **2019**, *81*, 696-702. [DOI: 10.1134/S1061933X19060103].